1355

FINAL TECHNICAL REPORT
GEORGIA TECH PROJECT A-1841

DETAILED DESIGN OF A 5 MWth SOLAR THERMAL TEST FACILITY

DESIGN AND TESTING OF THERMAL PROTECTION SYSTEMS FOR THE TEST TOWER

Subcontract To
Black and Veatch, Consulting Engineers
Kansas City, Missouri

Under Prime Contract To
Energy Research and Development Administration

By
S.H. Bomar, Jr.
L.G. Bias

October 18, 1976

1976

ENGINEERING EXPERIMENT STATION
Georgia Institute of Technology
Atlanta, Georgia 30332

Final Technical Report

DETAILED DESIGN OF A 5 MW_{TH} SOLAR THERMAL TEST FACILITY

DESIGN AND TESTING OF THERMAL PROTECTION SYSTEMS FOR THE TEST TOWER

Subcontract to

Black and Veatch, Consulting Engineers
Kansas City, Missouri

Under Prime Contract to

Energy Research and Development Administration

October 18, 1976

Authors

Steve H. Bomar, Jr.
Laura G. Bias

Engineering Experiment Station
Georgia Institute of Technology
Atlanta, Georgia 30332

Georgia Tech Project A-1841

ABSTRACT

The purpose of this program was to provide technical assistance in selection of thermal protection systems for the test tower of ERDA's 5 MWth Solar Thermal Test Facility (STTF). The STTF, now under construction at Albuquerque, New Mexico, will be used to test solar thermal conversion hardware using focussed solar radiation. It is possible that the concrete tower supporting the equipment under test can be illuminated by concentrated solar radiation, with structural damage resulting under certain conditions of incident flux and exposure time.

Experimental data were obtained on the response of several concretes to solar radiation at high incident flux levels; threshold fluxes to initiate damage were determined and rates of melting were measured. Design consultation was provided on the arrangement of metallic shielding systems.

TABLE OF CONTENTS

		Page
A.	INTRODUCTION	1
B.	PREPARATION OF CANDIDATE CONCRETE SPECIMENS	1
C.	PRELIMINARY SCREENING OF CANDIDATE CONCRETES	4
D.	TESTING OF RESPONSE OF CONCRETES TO CONCENTRATED SOLAR RADIATION	4
	1. Definition of Potential Hazards	4
	2. Experimental Facilities for Solar Testing	9
E.	RESULTS OF TESTS ON THE RESPONSE OF CONCRETES TO CONCENTRATED SOLAR RADIATION	13
	1. Qualitative Behavior	13
	2. Quantitative Measurements	16
	3. Heat Conduction Analyses of Concretes	24
	4. Rate of Melting Measurements	26
F.	ASSISTANCE ON METALLIC SHIELDING SYSTEMS	38

LIST OF ILLUSTRATIONS

		Page
1.	Horizontal-Axis Solar Furnace on Georgia Tech Campus	10
2.	Rear View of 60 cm (24 inch) Diameter Plexiglass Mirror Showing Vacuum Holding Fixture	11
3.	120 cm (48 inch) Diameter Plexiglas Mirror with Water Cooled Calorimeter at Focal Point	12
4.	Searchlight Parabolic Concentrating Mirror and Sample Holder	14
5.	Sample Holder for High Flux Tests (Note Calorimeter on Left and Specimen on Right)	15
6.	Typical Portland Cement Concretes Exposed to Concentrated Solar Radiation	17
7.	Calcium Aluminate, White Portland and Beige Portland Concretes Exposed to Concentrated Solar Radiation	18
8.	Internal Temperature at the Midplane of a Concrete Specimen Exposed to Concentrated Solar Flux	25
9.	Temperature Profile Beneath Surface of Semi-Infinite Slab-Plane Source	27
10.	Temperature Profile Beneath Surface of Semi-Infinite Slab-Point Source	28
11.	Rate of Melting Sample Positioned in Sample Holder at Focus of Solar Furnace	30
12.	Experimentally Measured Melting Rates for Concretes	32
13.	Rate of Melting Specimen, Concrete Specification 1	35
14.	Rate of Melting Specimen, Concrete Specification 4	35
15.	Rate of Melting Specimen, Concrete Specification 5	36
16.	Rate of Melting Specimen, Concrete Specification ABQ	36
17.	Rate of Melting Specimen, Concrete Specification S-33	37
18.	Calculated Tower Shield Performance	39

LIST OF TABLES

		Page
I.	SELECTION OF CANDIDATE CONCRETES FOR TESTING	2
II.	CONCRETE COMPOSITIONS/SPECIFICATIONS	3
III.	CHARACTERISTICS OF CONCRETE MIXES	5
IV.	EFFECT OF TEMPERATURE ON THE COMPRESSIVE STRENGTH OF CONCRETE COMPOSITIONS	6
V.	SAMPLE RESPONSE TO FOCUSSED RADIATION	19
VI.	"THRESHOLD FLUX" FOR CANDIDATE CONCRETES	21
VII.	RESPONSE OF THIN SAMPLES TO FOCUSSED RADIATION	23
VIII.	MELTING RATES FOR CONCRETES	31

A. INTRODUCTION

The purpose of this program was to provide technical assistance to Black and Veatch on selection of thermal protection systems for the test tower of ERDA's 5 MWth Solar Thermal Test Facility (STTF). The STTF is under construction at Albuquerque, New Mexico. When completed it will be used to test solar thermal conversion hardware using focussed, concentrated solar radiation. The hardware under investigation will be supported on a concrete tower and will be illuminated by radiation reflected by heliostats located on the ground. It is possible for the concrete tower itself to be struck by focussed radiation and it is therefore necessary to provide suitable thermal protection for the tower to prevent damage under these conditions.

The primary emphasis on this program has been collection of experimental data on the response of concretes to solar radiation at high incident flux levels. Such data have not been measured before, to the best of our knowledge. Tests have been conducted on concretes exposed to radiation from quartz lamps at high incident flux levels by Sandia Laboratories at Albuquerque and tests have been conducted on concretes exposed to flames; the results of the quartz lamp tests are briefly described in this report. Other tasks on this program included technical consulting on the design of metallic shielding systems.

B. PREPARATION OF CANDIDATE CONCRETE SPECIMENS

Seven candidate concretes were selected for possible application as thermal shielding materials on the STTF test tower; these are described in Tables I and II. They include three air-entrained standard gray concretes, a beige-colored concrete, a white-colored concrete, and two concretes based on high temperature refractory cements. All specimens were to be aged for 28 days prior to running any tests, so a list of specimen sizes was prepared and a complete set of specimens was cast for each "cement specification:"

40 each 2-inch diameter by 1.5-inch long,
10 each 6-inch diameter by 2-inch long, and
4 each 6-inch diameter by 12-inch long.

TABLE I

SELECTION OF CANDIDATE CONCRETES FOR TESTING

Cement Specification	Cement Type	Characteristics of Interest
1	IA (Gray Concrete)	Standard Portland Cement, Air Entrained
2	IIIA (Gray Concrete)	High Early Strength Portland Cement, Air Entrained
3	IA	Same as Specification 1 with Expanded Shale Aggregate
4	IA (Trinity Warmtone)	Standard Portland Cement, Air Entrained, with Beige Color
5	IA (White Portland)	Portland Cement, Air Entrained, White Color
6	Fondue Calcium Aluminate	High Temperature Cement, Expanded Shale Aggregate
7	Fondue Calcium Aluminate	High Temperature Cement, Crushed Firebrick and Expanded Shale Aggregate

TABLE II

CONCRETE COMPOSITIONS/SPECIFICATIONS

Cement Specification[1]	Cement Type[2]	Aggregate[3]		Cement Content[4] (lb/yd^3)
		Fine	Coarse	
1	IA	Sand	Granite	639
2	IIIA	Sand	Granite	639
3[5]	IA	Expanded Shale	Expanded Shale	640
4	IA Trinity Warmtone	Sand	Granite	639
5	IA White Portland	Sand	Granite	639
6[5]	Fondue Calcium Aluminate	Expanded Shale	Expanded Shale	709[6]
7[5]	Fondue Calcium Aluminate	Crushed Fire-Brick	Expanded Shale	709[6]

Notes:
1. Per correspondence JDW and JCG on 4/23/76.
2. ASTM C150-74.
3. ASTM C33-74.
4. ACI 211.1-74.
5. ACI 211.2-69.
6. Per correspondence JCG and JFD on 5/19/76; increase to develop desired slump.

The samples were cast in accordance with applicable ASTM procedures wherever possible, although minor deviations were necessary in some cases to obtain successful castings. All samples were then covered with polyethylene film and aged for 28 days at room temperature. The characteristics of the seven concrete mixes are shown in Table III.

C. PRELIMINARY SCREENING OF CANDIDATE CONCRETES

The first test to which the seven concretes were subjected was measurement of strength degradation after exposure to elevated temperatures. Four ASTM concrete compression specimens had been prepared for each concrete mixture. One of these was set aside as a control specimen and the other three were placed in a furnace, heated slowly to a specified temperature, held for four hours at temperature, and cooled slowly to room temperature. All "elevated temperature" specimens at a particular temperature were heated together and no samples were heated more than one time.

The control and heated specimens were then tested to failure in axial compression; test results are shown in Table IV. On the basis of the strength test results four concrete mixes were selected for further evaluation using concentrated solar radiation; two were identified as being primary candidates. These selections, made by Black and Veatch and Georgia Tech were:

Primary--Cement Specification 1 (Portland cement, sand and granite)
Cement Specification 4 (Trinity Warmtone, sand and granite)
Secondary--Cement Specification 2 (Hi-early Portland, sand and granite)
Cement Specification 5 (White Portland, sand and granite).

D. TESTING OF RESPONSE OF CONCRETES TO CONCENTRATED SOLAR RADIATION

1. Definition of Potential Hazards

The cases in which concentrated solar radiation can strike the tower were defined by Black and Veatch in a memorandum dated August 5, 1976:

> At the outset, it is necessary to define carefully the conditions under which solar radiation is expected to strike the tower. The most important cases are:

TABLE III

CHARACTERISTICS OF CONCRETE MIXES

Cement Specification[1]	Concrete Unit Weight[2]	Aggregate Unit Weight[3]			Yield[2]	Relative Yield[2]	Actual Cement Content[2]	Slump[4]	Entrained Air[5]
		Fine	Coarse	Blend					
	(lb/yd^3)	(lb/ft^3)	(lb/ft^3)	(lb/ft^3)	(ft^3)		(lb/yd^3)	(in)	(%)
1	132	---	---	112	1.58	1.05	610	5	6.25
2	139	---	---	112	1.50	1.00	639	3	5.50
3	98	66.4	56.9	---	0.86	0.86	744	3	8.25
4	141	---	---	112	1.48	0.98	648	3	6.00
5	134	---	---	112	1.57	1.05	610	5	6.50
6	105	66.4	56.9	---	0.95	1.05	746	3	---
7	107	67.1	56.9	---	0.93	1.08	762	3	---

Notes:
1. Per correspondence with JDW and JCG on 4/23/76.
2. ASTM C138-75.
3. ASTM C29-71.
4. ASTM C143-74.
5. ASTM C173-75.

TABLE IV

EFFECT OF TEMPERATURE ON THE COMPRESSIVE STRENGTH OF CONCRETE COMPOSITIONS

Cement Specification[1]	Compressive Strength[2] (psi)			
	Standard	600° F	800° F	1100° F
1	4067	3108	2600	1203
2	5705	5174	3742	2638
3	4096	2752	2172	1447
4	6306	5379	4230	2752
5	5341	4184	3116	1740
6	1744	1118	796	---[3]
7	2228	1779	1033	898

Notes: 1. Per correspondence JDW and JCG on 4/23/76.

2. ASTM C192-69.

3. Too fragile to test.

Normal Operation

(Defined as testing at any of the designated test levels and ports with properly focussed and tracking heliostats. Solar radiation striking the tower arises from spillage due to the concentrated solar image being larger than the test opening.)

1. Field zone A (78 heliostats, N-field) aimed at the 140 foot test level and onto the aperture of the 1 MW Martin-Marietta bench model receiver.

2. Field zones A and B (full north field) aimed onto the 5 MW Martin Marietta and McDonnell-Douglas receiver apertures.

3. Field zones A, C, D and E (360^{o} field) aimed into the aperture of the Honeywell receiver.

4. Field zones C or E aimed into the knockout panels on the east and west sides of the tower.

5. Heliostat stowage, emergency or otherwise.

Abnormal Operation

(Defined as equipment malfunction or operator error.)

1. Loss of power to heliostats. All heliostats are locked in position and the concentrated solar image moves off target as the sun continues to move. The important cases are:

   - o Zones A and B (entire N-field) aimed into 140 foot test level
   - o Zone C or E aimed into a knock-out panel

2. Zones A and B (entire N-field) incorrectly aimed at north tower face between levels 160 feet and 200 feet.

3. A single misaligned (but tracking) heliostat resulting in a single image striking the tower at a single, random position.

Other special cases may arise, but these are believed to bracket the important cases.

To properly address the problems of thermal protection, it is necessary to know (1) the distribution, flux maps, of concentrated solar flux on the tower for the cases listed in Section I, (2) the response of various concrete mixes when exposed to different solar flux levels, and (3) the degradation in strength of reinforced concrete as a function of temperature.

By "response" under (2) is meant surface melting, erosion or cracking and the temperature of the concrete as a function of time and distance from the exposed face. Except for data in the literature on the strength of some concrete mixes at elevated temperature, none of the above data was available to Black & Veatch when work began on tower design in April 1976.

Flux Maps

Normal Operation

Spillage fluxes for Cases 1-5, Normal Operation, are summarized below:

Case 1 - No significant spillage flux

Case 2 - No significant spillage flux for the Martin-Marietta receiver. Maximum spillage for the MACDAC receiver is 7 kw/m^2 on the top 1.5 feet of the north face on June 21, 10 a.m.

Case 3 - If the base of the Honeywell receiver is 25 feet above the top of the tower, maximum spillage is 13 kw/m^2 on the top 1.5 feet of the south face on June 21, 10 a.m. Spillage on north, east and west faces is $\sim$9 kw/m^2 on the top 1.5 feet.

If the base of the receiver is 50 feet above the tower top, there is no significant spillage.

Case 4 - Maximum spillage is 60 kw/m^2 at top and bottom of knock-out panel.

Case 5 - Not calculated. Result would depend on stowage procedure and could be minimized by stowing a few heliostats at a time in any given field sector.

Abnormal Operations

Flux maps for the Cases 1-3, Abnormal Operation, were determined recently by Sandia Albuquerque and pertinent values were transmitted verbally by telephone to Black & Veatch on August 4, 1976.

Case 1a - Maximum flux density falling on tower at edge of opening, 140 foot level, varies from 900 kw/m^2 down to 700 kw/m^2 over a period of about 8 minutes.

Case 1b - Maximum flux density falling on tower at edge of knock-out openings varies from 500 kw/m^2 down to 250 kw/m^2 over a period of 5 minutes.

Case 2 - Maximum flux of 3200 kw/m^2 falls on north face between 160 and 200 foot levels continuously until error is corrected. (Additional Data: At a radius of 0.5 m from the center, the flux is 2000-2200 kw/m^2; at a radius of 1.0 m the flux is 700-750 kw/m^2; at a radius of 1.5 m, the flux is 230 kw/m^2.)

Case 3 - Maximum flux of $\sim$ 40 kw/m^2 from close-in heliostats anywhere on the tower.

2. Experimental Facilities for Solar Testing

Georgia Tech has available on campus a small solar furnace consisting of a tracking heliostat and fixed parabolic concentrator, accompanied by appropriate equipment for measuring heat fluxes, temperatures, solar insolation, etc. This installation is shown in Figure 1. In an attempt to obtain heat flux patterns on the specimens with small viewing angles, some effort was devoted to development of an auxiliary concentrator for the furnace using bent Plexiglas mirrors. The aluminized Plexiglas was cut to a circular shape and supported on a metal ring at the perimeter of the mirror; the space behind the mirror was placed under partial vacuum, causing the mirror to deflect to a concave shape. These mirrors proved capable of supplying fluxes up to about 100 kw/m^2 and were used for a series of concrete tests at this exposure level and lower. However, additional effort to achieve the more perfect mirror geometry required for higher concentrations was deemed prohibitive in cost, and tests at flux levels above 100 kw/m^2 were run with the parabolic searchlight mirror which is the standard concentrator for the furnace. The back side of a 60 cm (24 inch) diameter Plexiglas mirror is shown in Figure 2, and the reflecting side of a 120 cm (48 inch) diameter Plexiglas mirror is shown in Figure 3.

The data recording system was based on a small computer which read the values of the transducer outputs each five seconds and printed the average of these values every thirty seconds. The experimental data recorded were: (1) direct incident solar insolation, (2) incident flux at the focal point before and after the test, (3) backside thermocouple output, and (4) interior thermocouple output. In addition, front surface temperatures were ready by an infrared optical pyrometer operating at a wavelength of 6.2 micrometers.

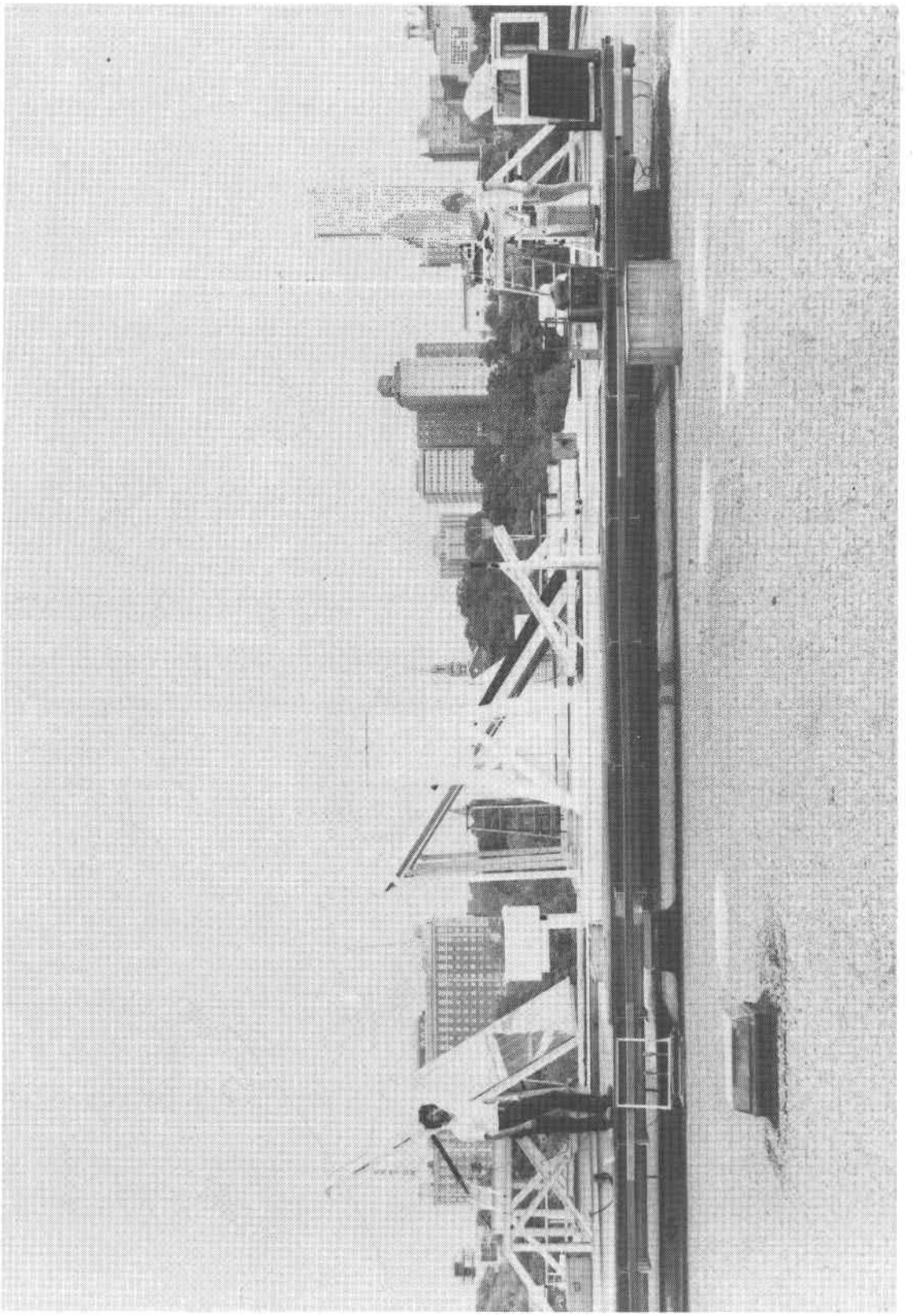

Figure 1. Horizontal-Axis Solar Furnace on Georgia Tech Campus.

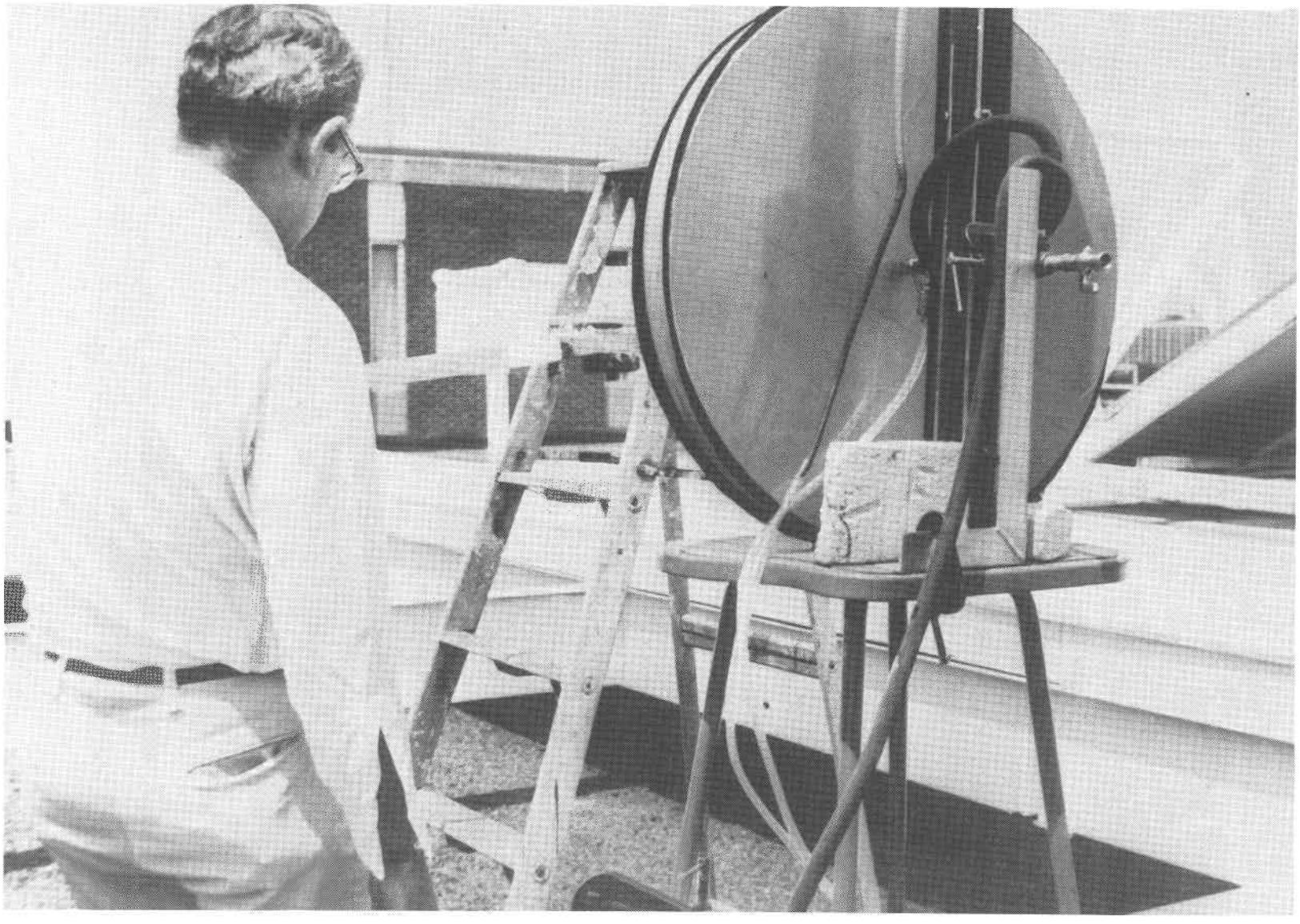

Figure 2. Rear View of 60 cm (24 inch) Diameter Plexiglass Mirror Showing Vacuum Holding Fixture.

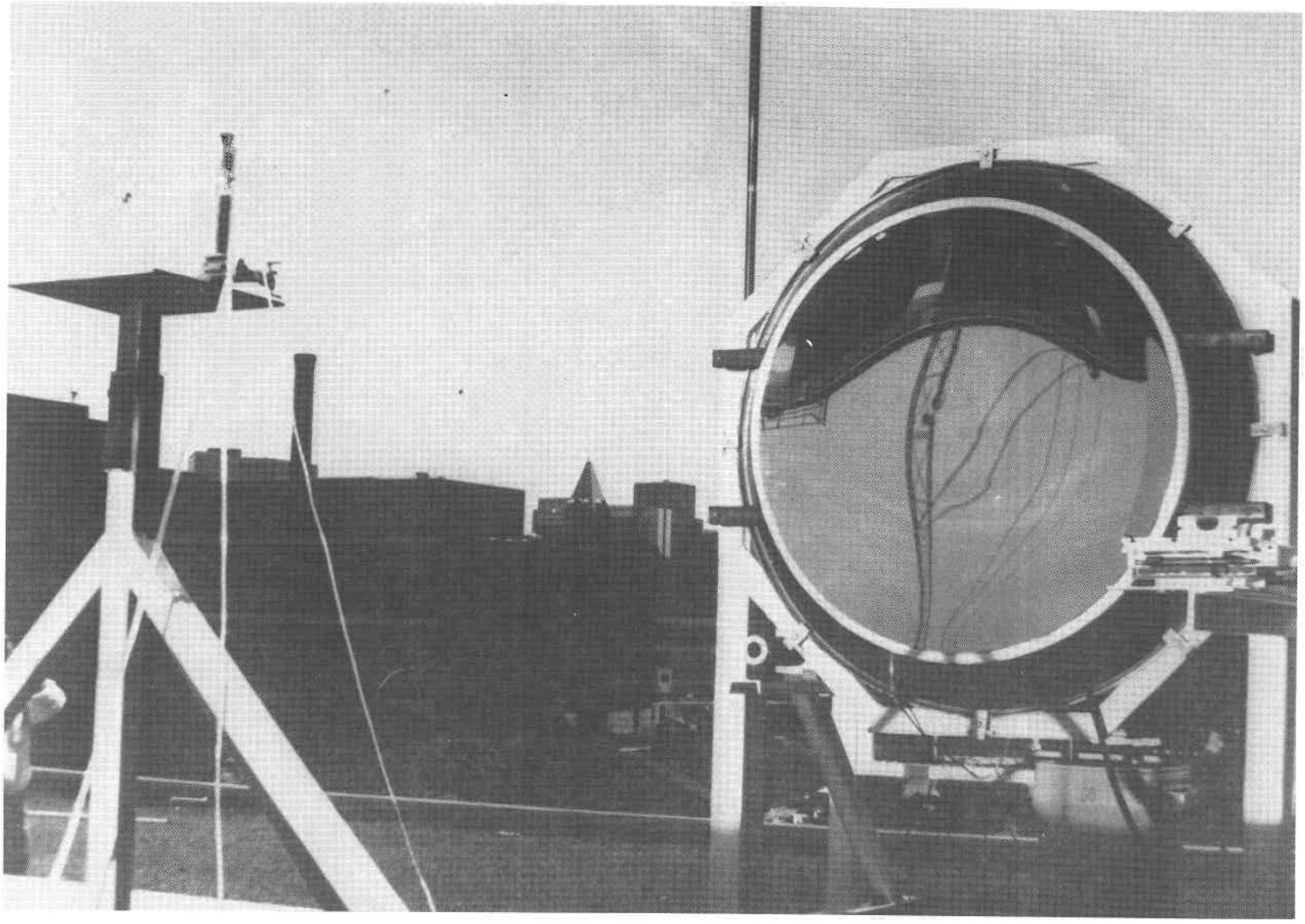

Figure 3. 120 cm (48 inch) Diameter Plexiglass Mirror with Water-Cooled Calorimeter at Focal Point.

Details of the specimen holder at the focus of the solar furnace can be seen in Figures 4 and 5. Figure 4 shows the parabolic mirror with the sample holder at the focus and Figure 5 shows a closeup photograph of the sample holder. The specimen and a calorimeter were mounted in a block of foamed fused silica; the silica block was arranged so that either the sample or the calorimeter could be placed in the focal point by sliding the block to the east or west against stops which positioned the block at the desired location. The sample is the larger diameter cylinder in the holding block.

The various types of concrete were exposed to incident fluxes ranging from 30 to about 2000 kw/m^2 in order to determine their responses to concentrated solar radiation; sample sizes for these tests were 5 cm (2 inch) diameter by 3.8 cm (1.5 inch) long. Subsequently tests were run on thinner samples at 5 cm diameter to approximate more closely the thickness-to-beam-diameter ratio anticipated on the structures of the STTF. Finally, a series of special tests was run to measure the melting rates of selected concretes.

E. RESULTS OF TESTS ON THE RESPONSE OF CONCRETES TO CONCENTRATED SOLAR RADIATION

1. Qualitative Behavior

Three typical Portland cement samples tested at increasing flux levels are shown in Figure 6 to illustrate qualitatively the appearance of damaged surfaces; the Cement Specifications 1 through 5 all behaved as shown, but the flux level at which damage occurred was dependent on the specimen material. The samples are 5 cm (2 inches) in diameter and the illuminated spot was about 2 cm (0.75 inch) in diameter. As seen in the left specimen of Figure 6, the first visible change in the concrete surface is a discoloration accompanied by minor cracking of the surface; a small melted area is also visible on this sample. At somewhat higher flux levels the melted area approached the beam diameter in size, as shown in the center sample. Finally, at still higher flux levels a molten crater was formed, as shown in the right sample. When the flux level was sufficiently high to cause melting, the melting occurred within about 10 seconds of the

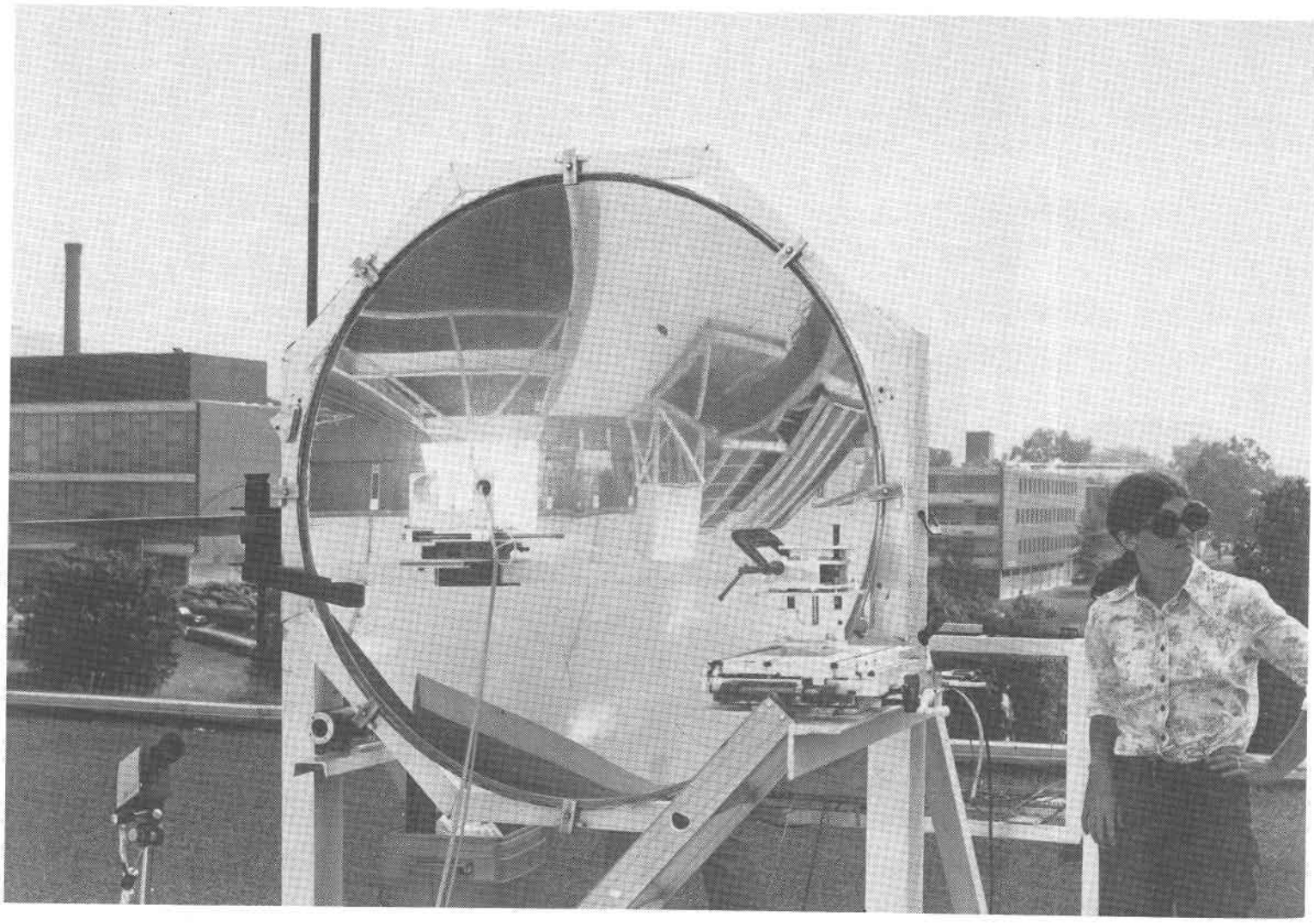

Figure 4. Searchlight Parabolic Concentrating Mirror and Sample Holder.

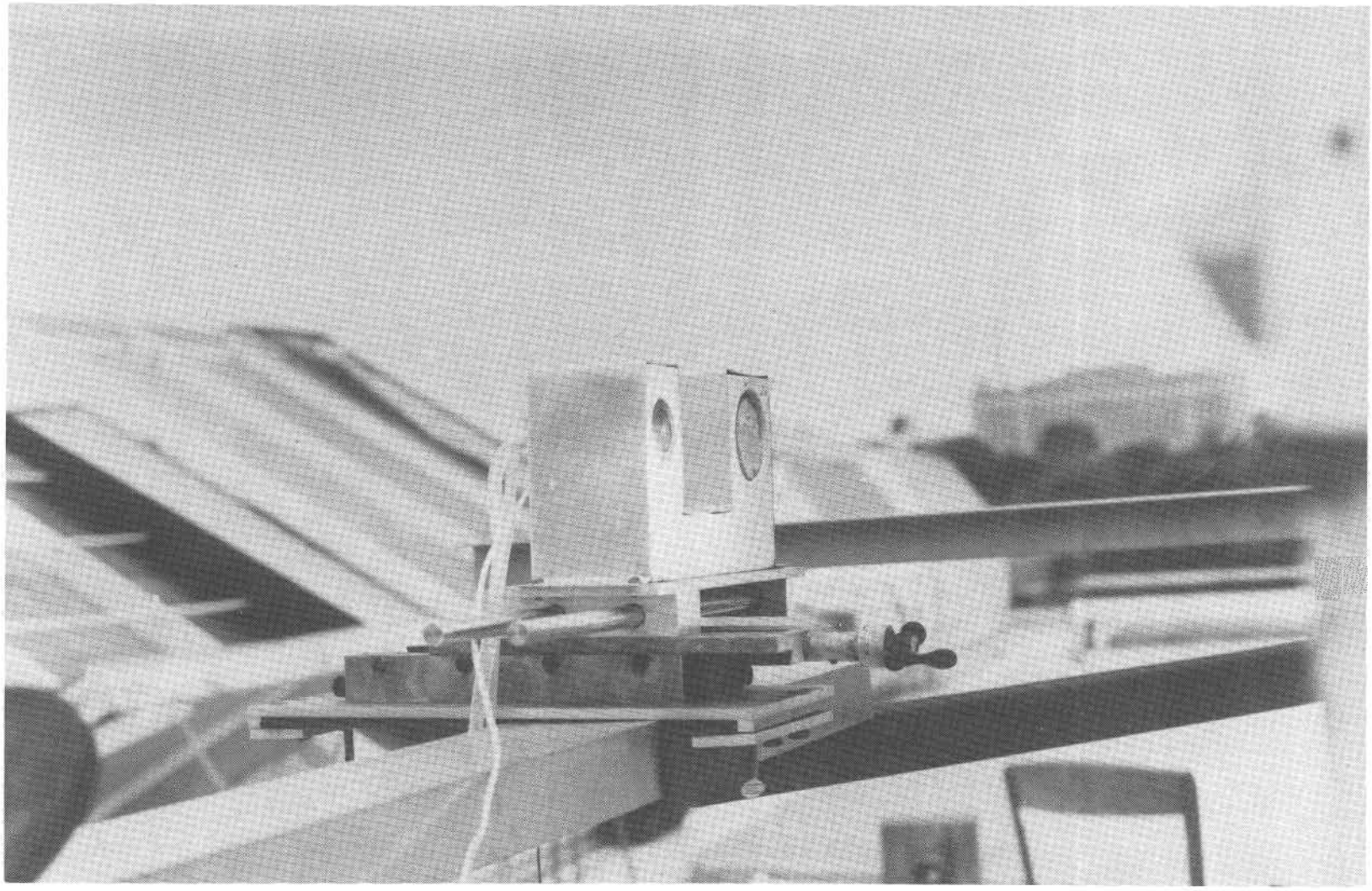

Figure 5. Sample Holder for High Flux Tests (Note Calorimeter on Left and Specimen on Right).

beginning of the exposure and subsequently no noticeable changes were visible when the samples were viewed through filtered glasses; all samples in Figure 6 were exposed for five minutes.

Three additional samples are shown in Figure 7 to illustrate qualitatively the behavior of different concretes. The left sample is Cement Specification 6 (calcium aluminate refractory cement with expanded shale aggregate); these materials melted at lower fluxes than Portland cement concretes and the rate of material removal at a given flux was estimated to be about three times as fast as with Portland cement concretes. The center sample is Cement Specification 5 (White Portland cement with sand and granite aggregate); this material was the most resistant to damage of all concretes tested, apparently because its white color gives a high diffuse reflectivity. The right sample is Cement Specification 4 (Trinity Warmtone with sand and granite aggregate); this material and the gray Portland cement concretes showed similar response to focussed solar radiation.

2. Quantitative Measurements

The first objective in the quantitative measurements program was to identify a "threshold flux to cause damage" for each of the concretes of interest (Cement Specifications 1, 2, 4 and 5). Determination of this "threshold flux" involved a degree of subjective judgment since it appeared that concretes might withstand a large number of exposures to fluxes which caused only surface discoloration and for engineering purposes such slight damage might be insignificant. However, surface melting clearly represented damage and the threshold flux must be somewhere between discoloration and melting. The threshold flux was chosen to be the lowest flux where significant surface cracking visible to the eye was detected.

Approximately 100 samples of the four concretes of interest were tested at various flux levels, most of these for exposure times of five minutes. The significant runs from this group are described in Table V; others were deemed unsuitable for various reasons such as equipment malfunction, interruption of insolation during the run, etc. This series of tests served to map the response of the candidate concretes over a wide range of incident fluxes and to permit identification of the threshold flux to cause damage for each concrete; the threshold fluxes are summarized in Table VI.

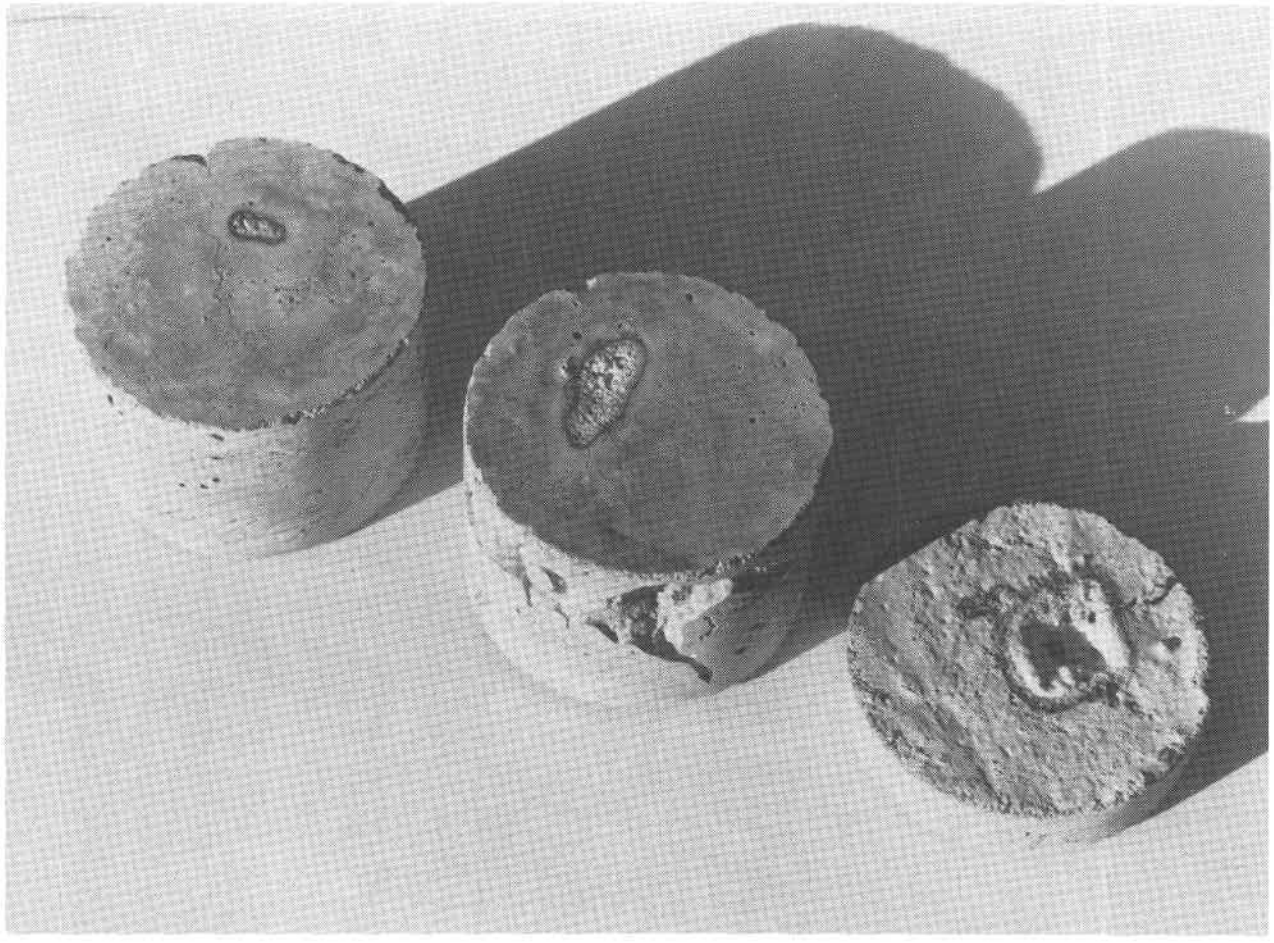

Figure 6. Typical Portland Cement Concretes Exposed to Concentrated Solar Radiation.

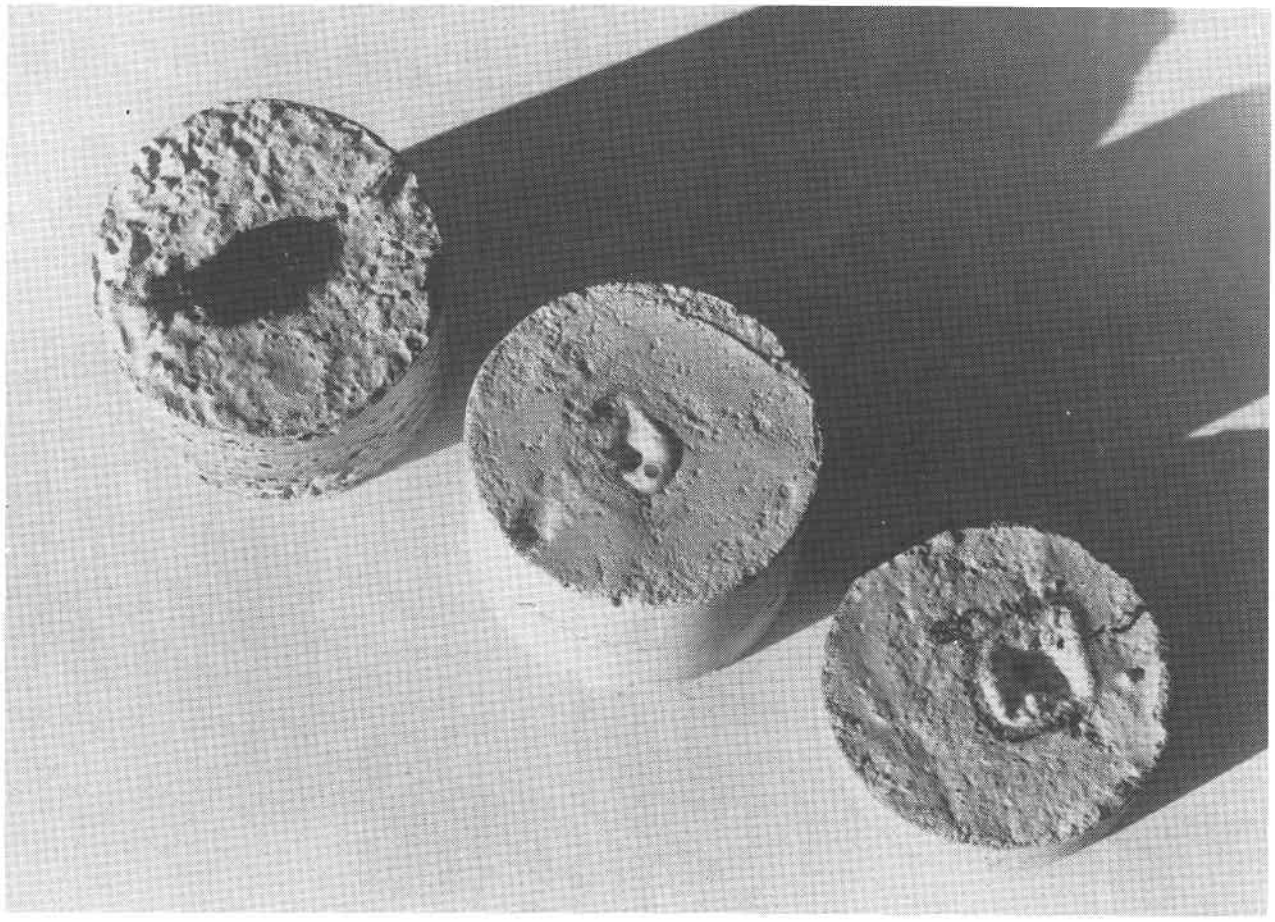

Figure 7. Calcium Aluminate, White Portland and Beige Portland Concretes Exposed to Concentrated Solar Radiation.

TABLE V

SAMPLE RESPONSE TO FOCUSSED RADIATION

SAMPLES 1-1/2 INCH THICK

Cement Specification	Cement Type (surface finish)	Flux & Time (kw/m^2; min)	Maximum Internal Temp (^oF)	Maximum Surface Temp (^oF)	Surface Damage
1	IA Portland				
	troweled	77;5	130	---	slight discoloration
	smooth	84;5	135	---	discoloration; surface cracking
	troweled	86;5	140	---	slight discoloration
	smooth	95;5 *	199	---	slight discoloration
	smooth	215;5*	202	---	discoloration; surface cracking
	smooth	370;5	213	1200	discoloration; cracking
	painted white	440;5	211	---	surface cracking
	smooth	600;5	210	900	melting
2	IIIA Portland				
	smooth	60;5*	135	---	discoloration; surface cracking
	smooth	104;5	194	---	discoloration
	painted white	240;5	---	---	no damage
	troweled	260;5*	216	---	discoloration; slight cracking
	smooth	368;5	210	1400	discoloration; cracking
	smooth	450;5	216	1625	discoloration; cracking

*Threshold flux.

(Continued)

TABLE V (Continued)

SAMPLE RESPONSE TO FOCUSSED RADIATION

SAMPLES 1-1/2 INCH THICK

Cement Specification	Cement Type (surface finish)	Flux & Time (kw/m^2; min)	Maximum Internal Temp (^oF)	Maximum Surface Temp (^oF)	Surface Damage
4	IA Trinity Warmtone				
	smooth	60;5	---	---	slight discoloration
	smooth	105;5*	130	---	discoloration; slight cracking
	smooth	520;5	---	1600	melting
	smooth	570;5	---	1350	melting; one deep hairline crack
5	IA White Portland				
	smooth	73;5	125	----	no damage
	smooth	69;5	130	---	no damage
	smooth	90;5	130	---	no damage
	smooth	225;5	180	---	no damage
	smooth	460;5	205	---	discoloration
	smooth	640;5*	198	---	discoloration; slight cracking
	troweled	1680;5	208	2225	melting; 0.15 inch hole

*Threshold flux.

TABLE VI

"THRESHOLD FLUX" FOR CANDIDATE CONCRETES*

Cement Specification	Description	Threshold Flux (kw/m^2)
1	Standard Portland with sand and granite	215
2	High Early Set Portland with sand and granite	60
4	Trinity Warmtone with sand and granite	105
5	White Portland with sand and granite	640

*5 minute exposures; 3.8 cm (1.5 inch) thickness.

Previous materials tests conducted by Georgia Tech at the CNRS Solar Furnace in France had shown that the behavior of ceramic materials in high radiant heat fluxes is strongly dependent on surface color. This characteristic was also observed in the concrete tests described herein. White materials exhibit a high diffuse reflectivity which causes these materials to reflect, rather than absorb, a large fraction of the incident radiation. (Very white high purity slip-cast fused silica was estimated to absorb on the order of 5 percent of the incident power.) A relatively slight darkening of the surface, for example changing from white to gray Portland cement, causes a substantial increase in surface absorptivity with an accompanying increase in vulnerability to damage by radiant energy. As noted earlier, when melting occurred it appeared visually to take place within about ten seconds after the start of the test and no further change was visually observed after this time. At incident fluxes up to about 800 kw/m^2, penetration of the melt into the sample surface was limited to one or two millimeters.

Two specimens are shown in Table V whose surfaces had been painted white with a high temperature paint. The purpose of these tests was to determine whether the white color would increase the "threshold flux." The white refractory paint was VHT SP-101 White, manufactured by Sperex Corporation,

2239 Pontius Avenue, Los Angeles, California 90064. In both cases the threshold flux appears to have been increased in comparison to an unpainted sample; the paint was not damaged until melting of the concrete occurred.

It was learned that Sandia Laboratories in Albuquerque, New Mexico had tested concretes in high radiant fluxes provided by infrared quartz lamps. Mr. Paul H. Adams furnished information on the tests which were conducted at the Sandia Radiant Test Facility:

> We have tested 12 concrete samples to incident radiant heat fluxes of 345, 672 and 1120 kw/m^2. All samples were 6" diameter by 3.15" long, cylindrically shaped. Temperatures were measured at depths of 1/4, 1/2, 3/4, 1, 1-1/2 and 2" from the heated surface. Aggregate in the concrete was basalt or limestone 3/8 inch or 1 inch maximum size. In all cases except for the lowest heat flux, melting of the surface of the concrete occurred. The specimen receiving the lowest heat flux for one hour exhibited no obvious evidence of damage during or immediately after the application of the radiant heat flux. However, after two weeks it was reexamined and found that the first 1/2 inch had been reduced to a loose powdery structure.

He reported further that the high-flux samples were run for a total time of ten minutes and that all samples which exhibited melting did so within 15 to 30 seconds after initiation of the radiant heat pulse; these Sandia data were in good agreement with observations on this program.

As results of the test program were being analyzed, a question arose as to whether sample thickness seriously influenced the response of concretes to focussed radiation. The 3.8 cm (1.5 inch) thick samples described above had a thickness-to-beam-diameter ratio of at least two while the STTF tower could be expected to have a ratio on the order of one-half to one. Several specimens were cut to thicknesses of 63 mm (0.25 inch) and 125 mm (0.5 inch) and tested at high incident fluxes to check the behavior of thin specimens. These data are shown in Table VII; if they are compared with the last entry in Table V it appears that sample thickness had no important influence on the tests. This result is reasonable since the tests were concerned primarily with surface phenomena.

At the conclusion of these basis tests to observe the response of concretes to high solar radiation fluxes, the following general observations could be made:

TABLE VII

RESPONSE OF THIN SAMPLES TO FOCUSSED RADIATION

Cement Specification	Cement Type (sample thickness)	Flux & Time (kw/m^2; min)	Maximum Internal Temp (^oF)	Maximum Surface Temp (^oF)	Surface Damage
1	IA Portland ½ inch	1835;15	---	2325	Hole melted to depth of 0.27 inches
4	IA Trinity Warmtone ¼ inch	1660;12	thermocouple melted	2575	Hole melted to depth of 0.12 inches

a. The mechanism for material removal appears to be melting rather than spalling of pieces from the concrete surface,

b. The melt is a viscous liquid which does not flow rapidly from the heated site,

c. The cement matrix appears to melt more readily than the aggregates in the concretes tested, and

d. The surface recession appears to be caused by absorption of molten material into the porous concrete structure and movement of material around the melt site, rather than gross removal of molten material from the surface by flow or vaporization.

3. Heat Conduction Analyses of Concretes

Since the structural strength of concrete deteriorates substantially at temperatures above 700 K (800^{o} F), the temperature profile within a structural wall is important. Temperature profiles can be calculated if surface temperatures and thermal properties of the concrete are known. Experimental data suggest that the surface melting temperature of concrete is in the range of 1500 to 1650 K (2200^{o} to 2500^{o} F) and the room temperature thermal properties are readily found in standard handbooks. However, the question remains whether the room temperature thermal properties are valid at high temperatures. For example, does chemically bound water in concrete absorb energy during vaporization at elevated temperatures and thereby cause the effective heat capacity to be different from the room temperature value? A brief study of these problems was undertaken to determine whether calculated temperature profiles match experimental temperature profiles.

A typical plot of internal temperature at the midplane of a concrete sample versus time is shown in Figure 8. Data of this type were measured for a number of samples. Then theoretical temperature profiles were calculated for two heat conduction models: plane wave heating on a semi-infinite slab and point source heating on a semi-infinite slab. The properties of concrete used for these calculations were:

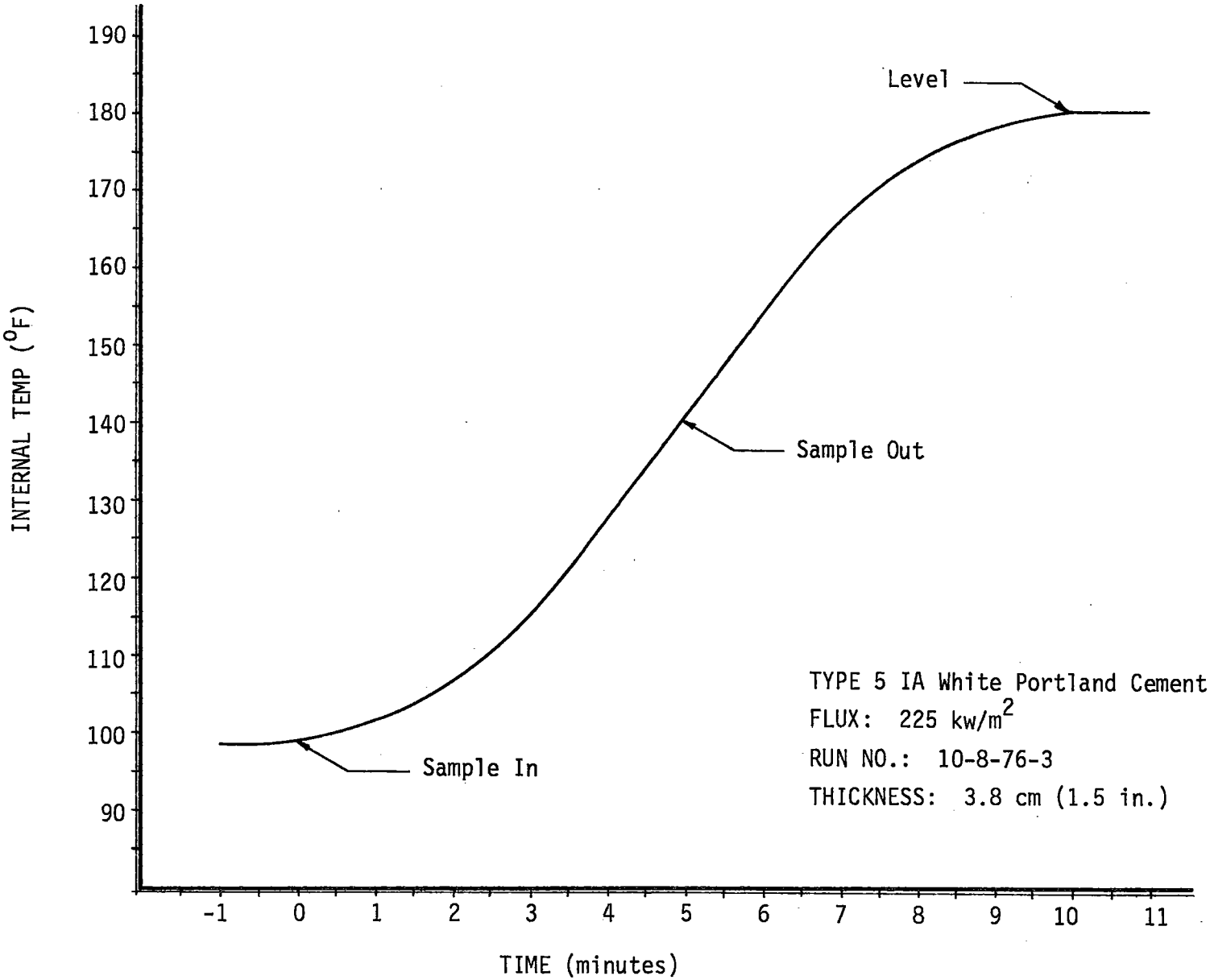

Figure 8. Internal Temperature at the Midplane of a Concrete Specimen Exposed to Concentrated Solar Flux.

density = 2.163 gm/cm^3

heat capacity = 0.239 cal/gm ^oC

thermal conductivity = 0.0025 cal/cm ^oC sec

thermal diffusivity = 4.84×10^{-3} cm^2/sec

The initial temperature data generated on this program did not compare well with the theoretically calculated profiles. In the plane wave case the experimental geometry did not match the model geometry because only a small fraction of the surface area of the sample was heated by the focussed solar radiation. In the point source case the rate of heat input to the sample at the point source was unknown, although comparison of measured and calculated temperatures suggested that the heat input had been on the order of 25 to 50 watts. (The incident power on the sample was estimated to be about 1100 watts.) However, experimental temperature profile data furnished by Mr. Paul Adams for the Sandia concrete tests showed reasonably good agreement with calculated profiles when the position of the sample surface was adjusted to account for recession of the surface plane. The calculated temperature profiles with a Sandia profile added are shown in Figures 9 and 10.

4. Rate of Melting Measurements

After the basic behavior of the selected concretes in high solar radiant energy fluxes had been determined, the more specific question of rate of melting was addressed. The purpose of this work was to obtain data needed for estimating the lifetime of a concrete shield under exposure to various heat fluxes; the desired output of the task was a set of curves showing rate of surface recession versus incident flux.

Two types of refractory cements manufactured by Sauereisen Cements Company of Pittsburgh, Pennsylvania and a concrete prepared by a contractor in Albuquerque, New Mexico were added to the list of specimen materials. The Sauereisen specimens were identified by the designations S-33 and S-72, corresponding to the manufacturer's product code; they were reported to be cast materials identical in composition to gunited materials proposed for use on the STTF tower. The specimens cut from the block of concrete sent from Albuquerque were identified by the designation ABQ and the

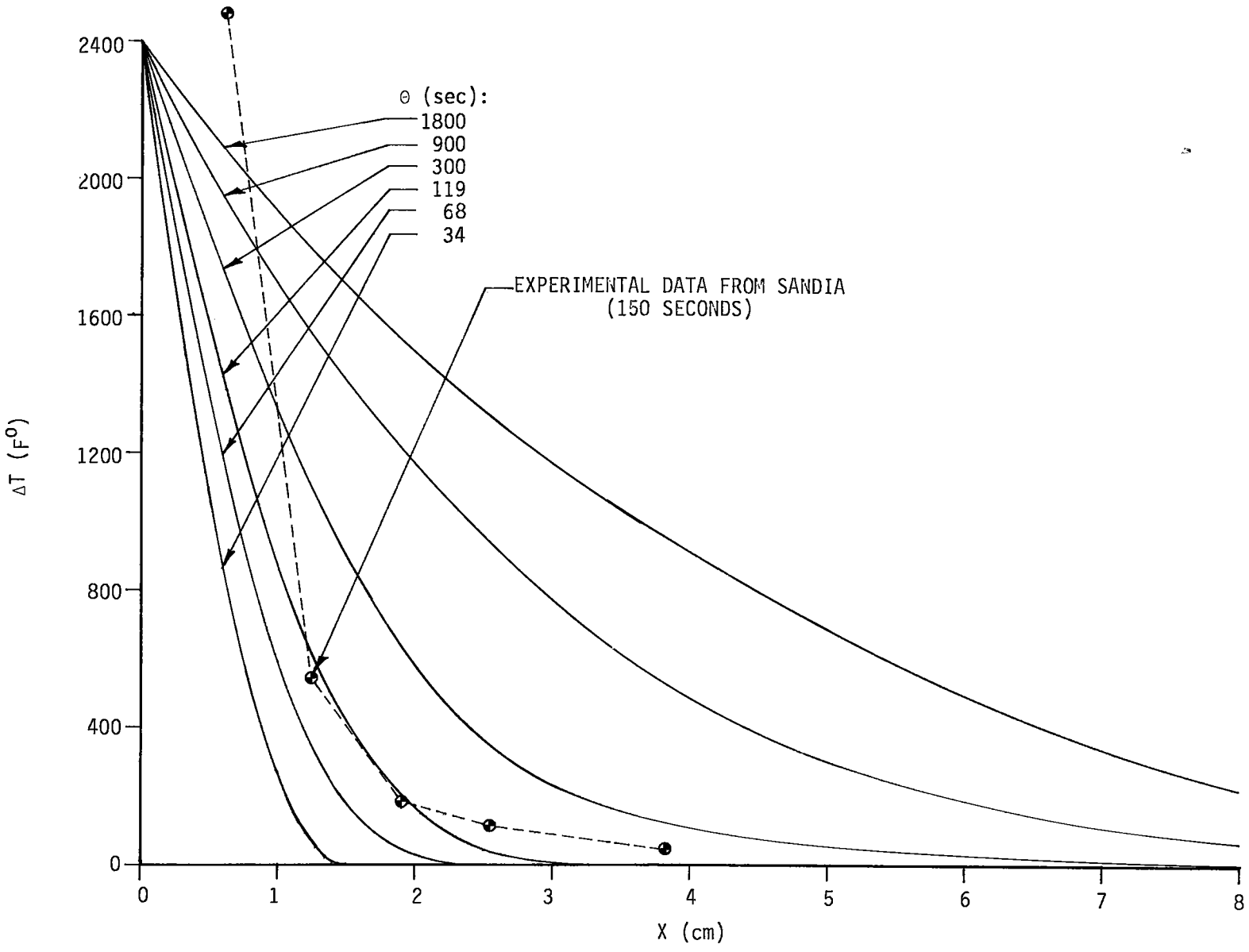

Figure 9. Temperature Profile Beneath Surface of Semi-Infinite Slab-Plane Source.

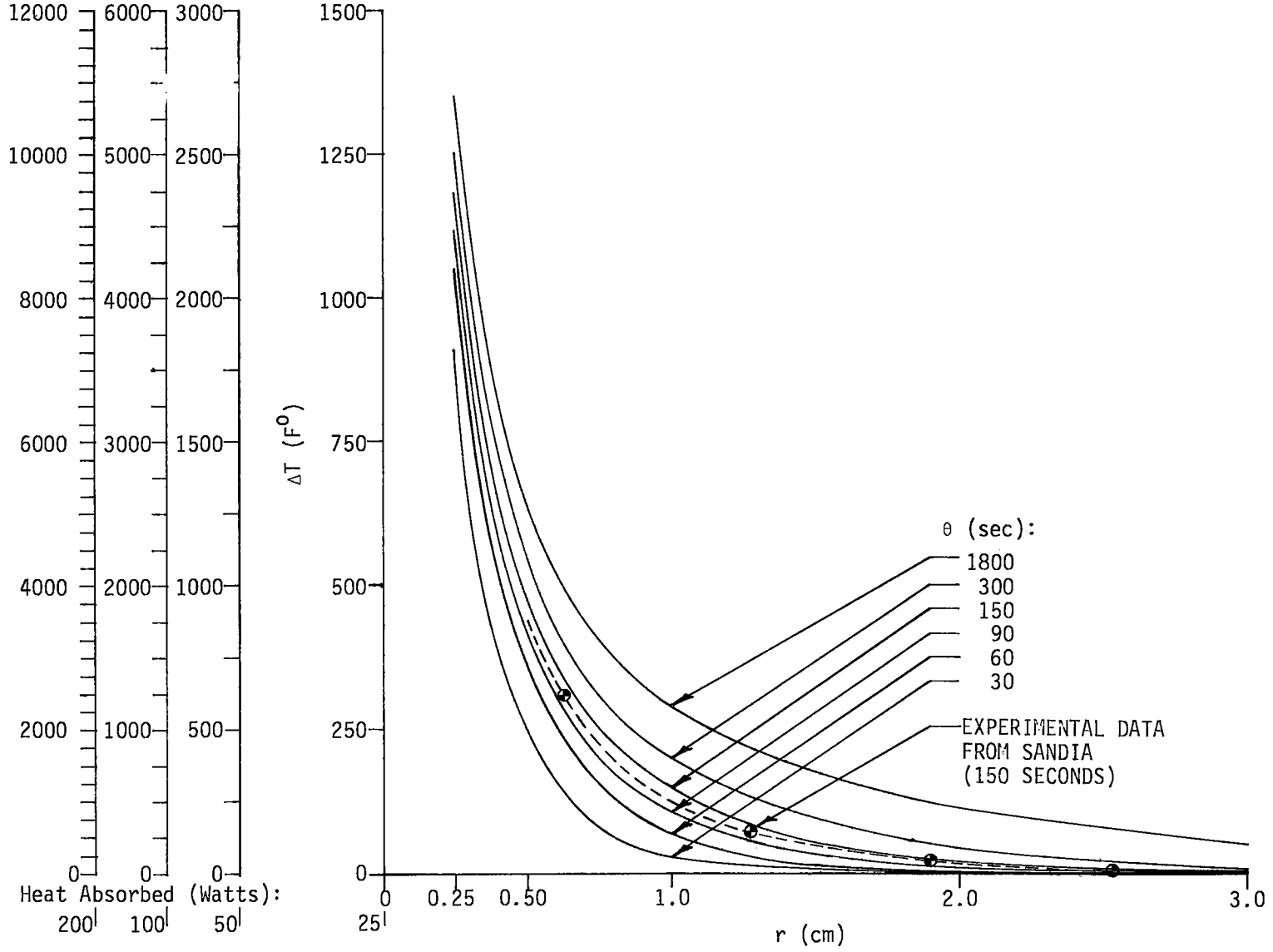

Figure 10. Temperature Profile Beneath Surface of Semi-Infinite Slab-Point Source.

specimens prepared by Georgia Tech were identified by the Cement Specification numbers used throughout this report.

In order to prevent radial heat conduction in the rate of melting specimens it was decided that the exposed area of the samples should be comparable in size to the incident focussed beam. Also, the samples should be moved toward the parabola during testing so that the melting front remained in the focal plane as closely as possible. To accommodate these requirements the samples were sawed from larger pieces to obtain a cross section approximately 2 cm (0.75 inch) square and the sample holder on the solar furnace was modified, as shown in Figure 11, by the addition of a cylindrical plug with a square hole at its center. The square sample in Figure 11 has been moved forward from the focal plane so that it can be readily identified in the photograph. The samples were moved manually during the tests so that their melting surfaces remained approximately in the focal plane. (The complete sample holder can be seen in Figure 5.)

Melting rates were determined by dividing the test time into the melted distance; the melted distance was taken to be the difference between the original sample length and the unmelted length after the test. The test procedure was first to measure the incident flux at the focal point using a water-cooled disk calorimeter, then move the sample into the focal point, push the sample forward to maintain the melting front in the focal plane, and finally to move the calorimeter into the focal point again. The exposure times for the Georgia Tech and Albuquerque specimens was three minutes; the exposure times for the Sauereisen samples was one minute. The experimental data on melting rates are given in Table VIII and Figure 12.

Certain qualitative observations were made during the testing which may be of interest but are not conveniently documented in a figure or table:

1. In addition to surface darkening, a bubbling phenomenon was usually observed upon melting, presumably due to the evolution of trapped gases. The bubbling occurred within a few seconds after the samples were placed in the focus of the concentrating mirror; it was much more pronounced in the Sauereisen materials

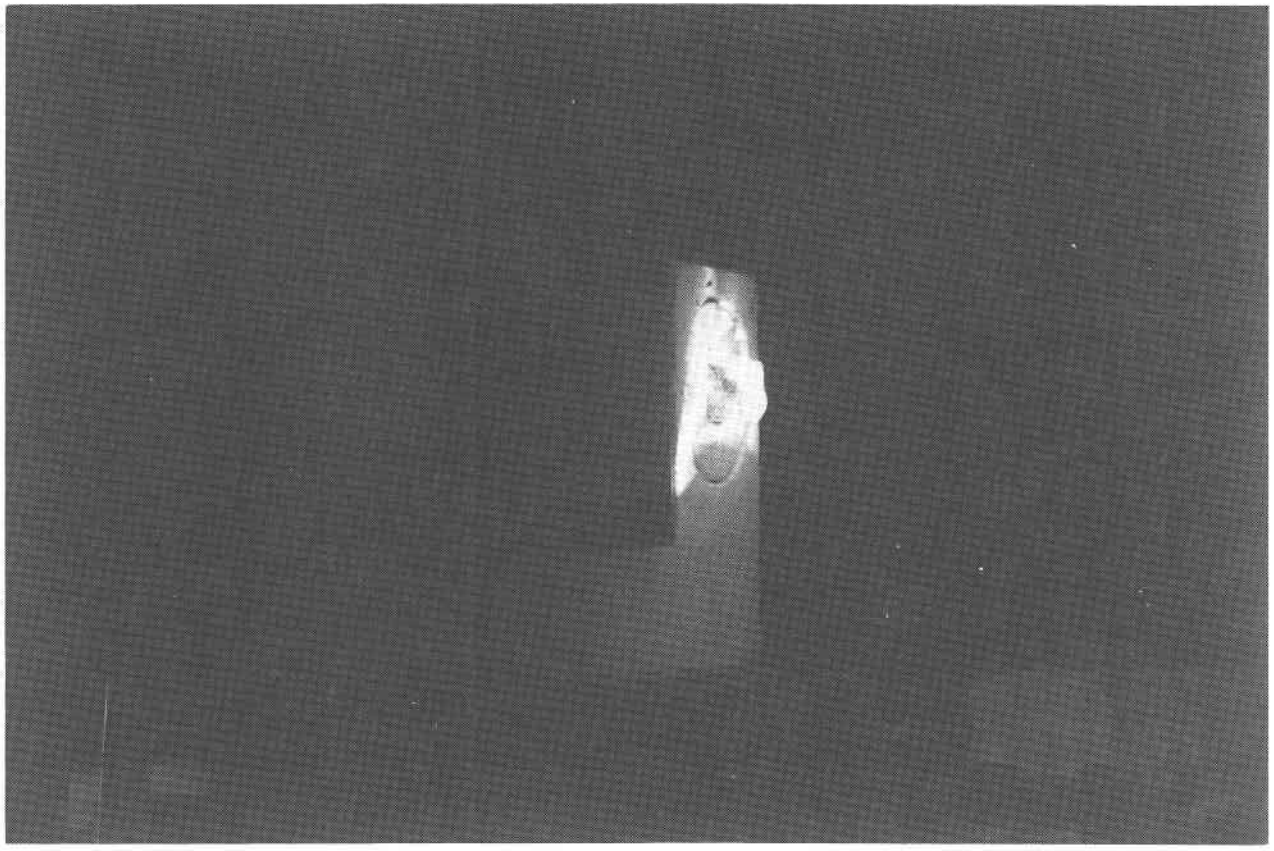

Figure 11. Rate of Melting Sample Positioned in Sample Holder at Focus of Solar Furnace.

TABLE VIII

MELTING RATES FOR CONCRETES

Concrete Type	Front Cross Section (height (in) x width (in))	Flux (kw/m^2)	Melt Rate (in/min)
1	0.62 x 0.62	1200	0.04
1	0.67 x 0.92	1730	0.25
1	0.56 x 0.50	1795	0.13
1	0.95 x 0.98	1845	0.17
4	0.50 x 0.50	1267	0.05
4	0.62 x 0.60	1715	0.08
4	0.53 x 0.55	2050	0.25
5	0.58 x 0.62	1113	0.03
5	0.87 x 0.81	1600	0.07
5	0.56 x 0.56	1785	0.11
ABQ	0.86 x 0.86	1000	0.06
ABQ	0.80 x 0.78	1480	0.05
ABQ	0.50 x 0.50	1910	0.10
S-33	0.60 x 0.66	953	0.28
S-33	0.58 x 0.56	1394	0.40
S-33	0.67 x 0.60	1473	0.61
S-33	0.75 x 0.50	1575	0.33
S-33	0.69 x 0.51	1780	0.26
S-33	0.57 x 0.57	2069	2.32
S-72	0.73 x 0.69	648	0.27
S-72	0.62 x 0.60	1370	0.17
S-72	0.63 x 0.44	1795	0.61
S-72	0.59 x 0.50	1990	0.79

and appeared to involve more depth of material than in the Portland samples.

2. The concretes tended to melt faster around the edges of the specimens, where they were not insulated, than in the center of the specimens. Thus, the final shape tended to round on the exposed end rather than flat and square.

3. The cement matrix tended to melt around the aggregate initially and then the aggregate began to melt at a much slower rate. This was observed in all samples, regardless of aggregate size.

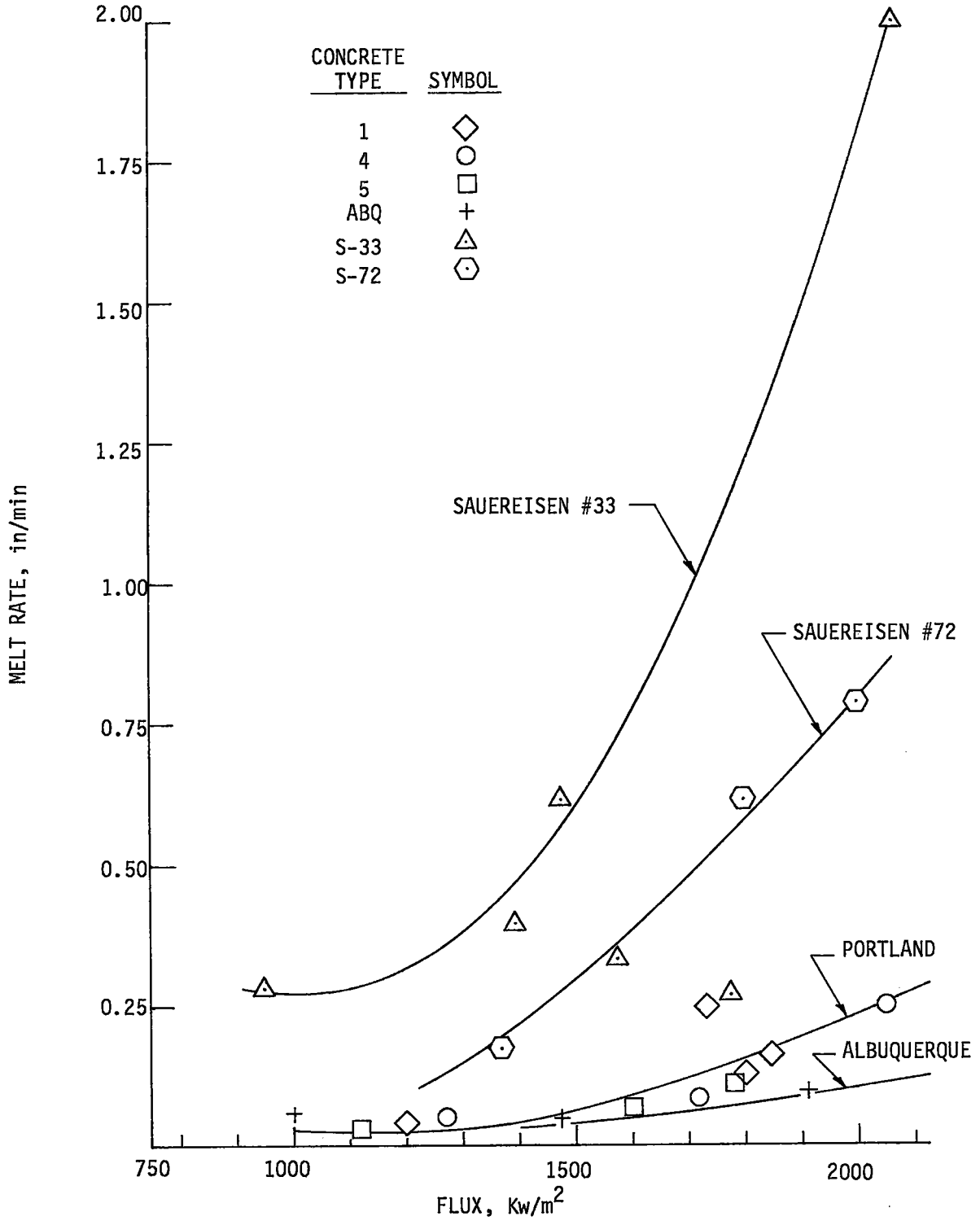

Figure 12. Experimentally Measured Melting Rates for Concretes.

4. The Albuquerque samples were the only ones that had exposed aggregate on their surfaces. The front of these samples cracked off during handling several days after testing. This deterioration after testing was also observed by Sandia investigators and reported to us by Paul Adams in his letter of July 29, 1976. This did not occur with either the Portland or Sauereisen samples. It appears that the cement matrix melted around the aggregate, although the disintegration of the samples did not occur for several days.

5. During testing the molten material did not drip off the samples; it tended to flow away from the melt zone and thereby change the position of the molten front.

6. When the samples were removed from the holder after the tests it was noticed that the Sauereisen materials were much cooler than the Portland or Albuquerque materials. The heated end of the Sauereisen samples could be handled within five minutes after the test, whereas it took about 30 minutes for the Portland and Albuquerque samples to become cool enough to handle. This suggests that the Sauereisen samples had a lower melting point than the others.

7. The attached plot of melting rate versus incident flux for all the specimens tested shows that the melting rate increases in an exponential fashion with increasing flux. All the Portland-based cements seem to fall in a group once a flux sufficiently high to cause melting has been reached. The two Sauereisen cements melt much more rapidly than Portlands at any given flux level. All our measurements together indicate that surface color is a controlling factor in initiation of melting, but that other material properties control the rate of melting after melting begins.

8. Several samples were subjected to repeated exposures to concentrated solar fluxes in order to determine whether their

responses changed as the number of exposure cycles increased. No response changes could be detected.

Photographs of representative rate of melting specimens are shown in Figures 13 through 17. Evidence of bubbling can be seen in the Portland cement concretes (Cement Specifications 1, 4 and 5). The Albuquerque specimen has sharp edges rather than the melted appearance of the other materials; this is a result of crumbling of the specimen after the run. The Sauereisen specimen has a large hollow bubble at the molten surface and darkening for a considerable distance into the sample.

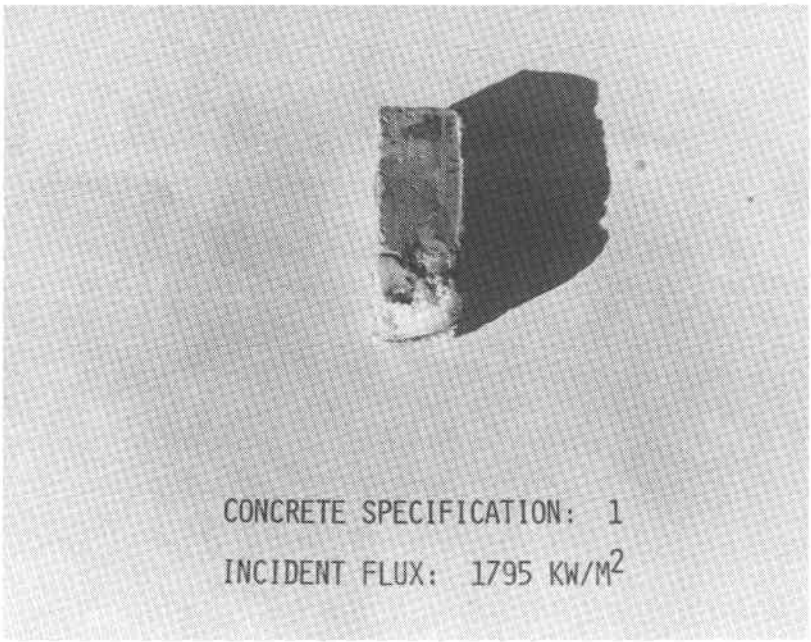

Figure 13. Rate of Melting Specimen, Concrete Specification 1.

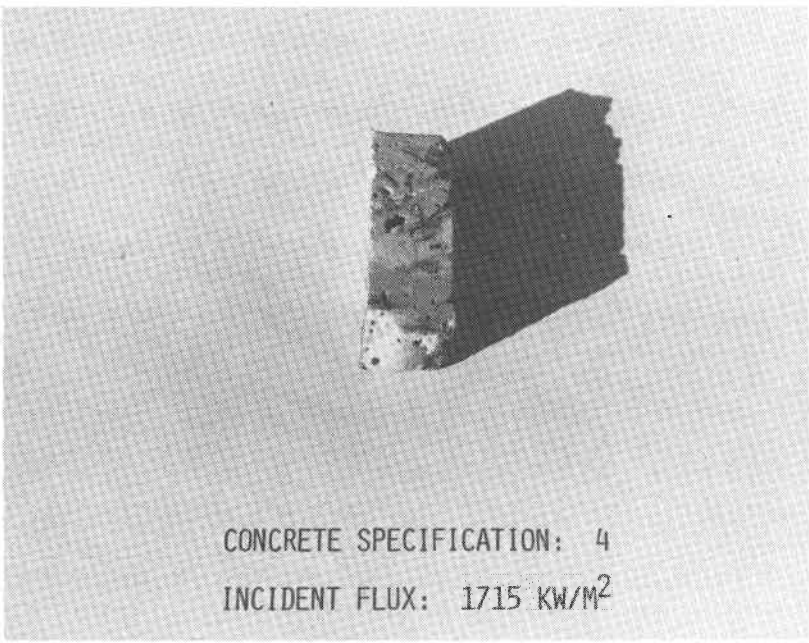

Figure 14. Rate of Melting Specimen, Concrete Specification 4.

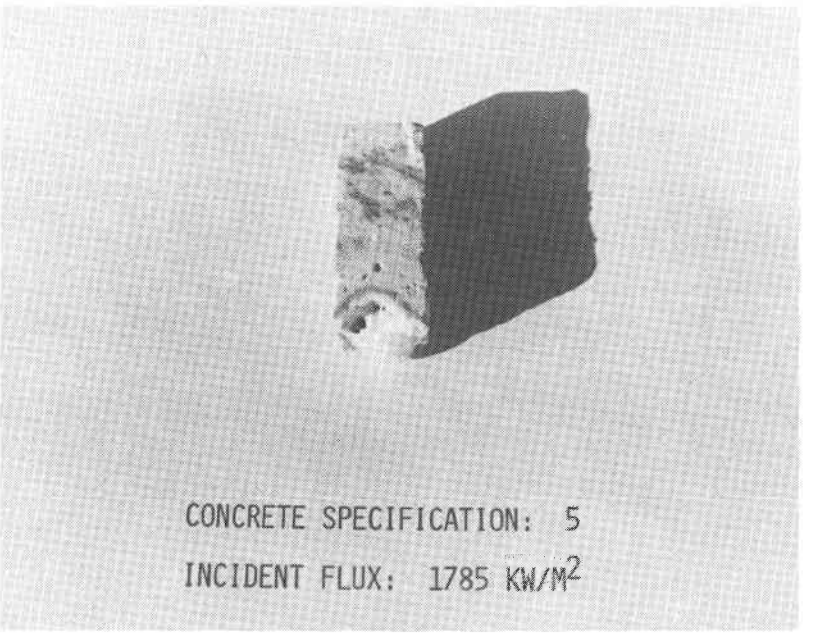

Figure 15. Rate of Melting Specimen, Concrete Specification 5.

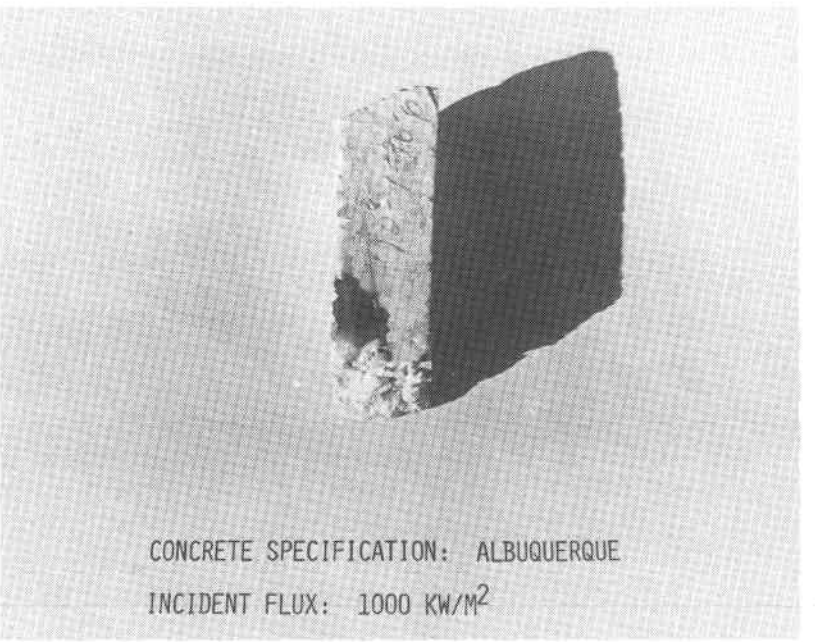

Figure 16. Rate of Melting Specimen, Concrete Specification ABQ.

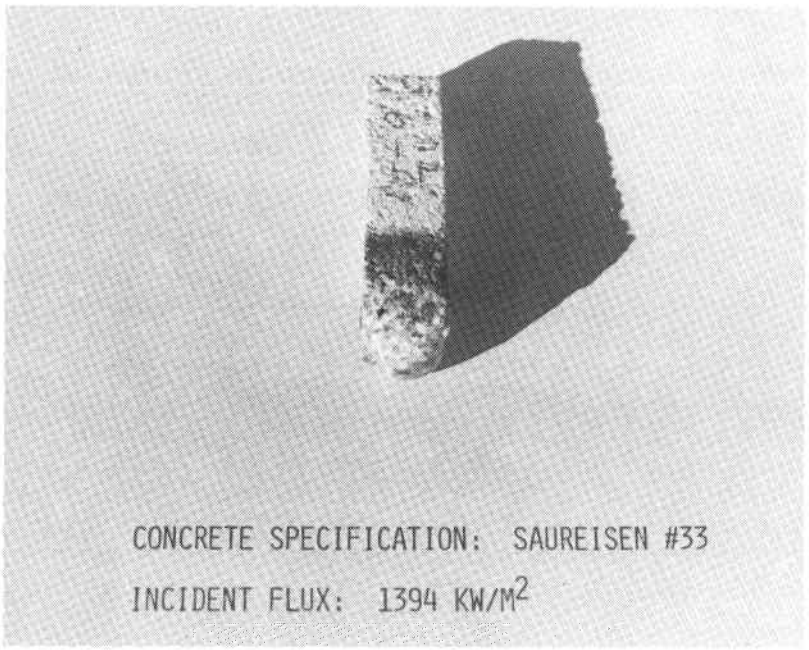

Figure 17. Rate of Melting Specimen, Concrete Specification S-33.

F. ASSISTANCE ON METALLIC SHIELDING SYSTEMS

The purpose of this task was to provide assistance on specific problems at Black and Veatch's request. The activities consisted of commenting and advising on designs, performance of calculations, and similar work of a consulting nature:

1. One early shield design was referred to Georgia Tech for comments; Georgia Tech recommended lengthening of louvered panels in order to eliminate horizontal gaps through which radiation could reach the tower structure.

2. Georgia Tech was asked to recommend a high temperature white paint suitable for use on metallic shields; we suggested Sperex VHT SP-101 White paint manufactured by Sperex Corporation, 2239 Pontius Avenue, Los Angeles, California 90064.

3. Georgia Tech was asked to comment on the substitution of low-alloy steel for stainless steel on the metallic shielding in order to reduce costs. We believe this approach is feasible but the low-alloy steel must be painted on both sides to prevent corrosion. The stainless steel would require painting only on the side exposed to radiation. We recommended that the exposed side be painted with Sperex VHT SP-101 White to obtain a high diffuse reflectivity and the reverse side be painted with Sperex VHT SP-117 Aluminum to obtain a low emissivity.

4. Georgia Tech was asked to estimate the energy flux radiated to the tower using a single layer of stainless steel shielding. A plot showing tower shield performance is given in Figure 19. These curves are based on the use of Sperex SP-101 White VHT paint on the exterior of the stainless steel shield and a mill finish on the interior. It was assumed that the interior surface of the stainless steel becomes fully oxidized at 700^{o} F. Performance equal to this could be obtained with plain carbon steel by painting the shield exterior with SP-101 White and the interior with SP-117 Aluminum.

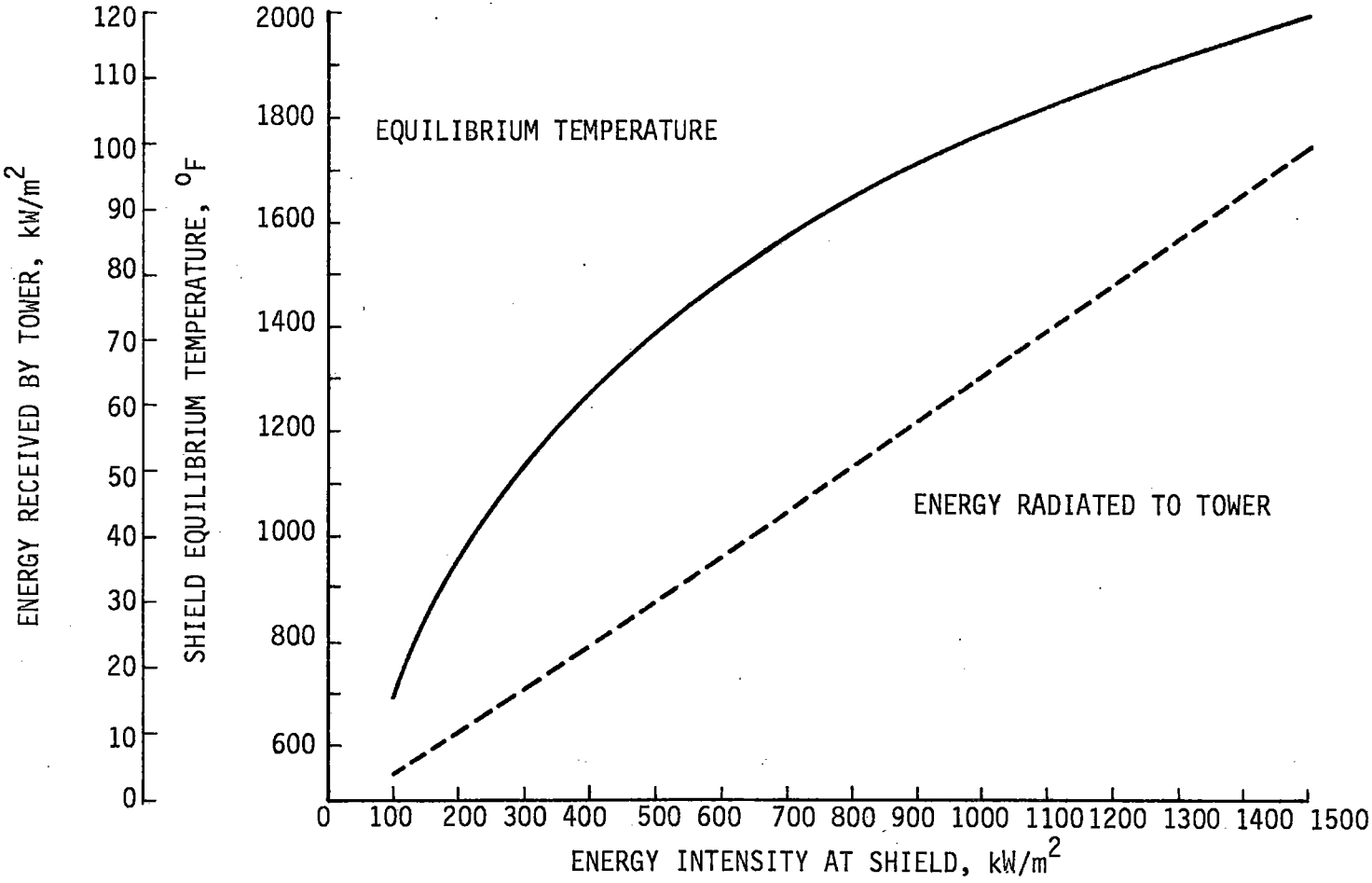

Figure 18. Calculated Tower Shield Performance.